



Biosorption of Cr(VI) on immobilized *Hydrilla verticillata* in a continuous up-flow packed bed: prediction of kinetic parameters and breakthrough curves

Santhi Raju Pilli, Vaibhav V. Goud, Kaustubha Mohanty*

Department of Chemical Engineering, Indian Institute of Technology Guwahati, Guwahati 781039, Assam, India
Tel. +91 361 2582267; Fax: +91 361 2582291; email: kmohanty@iitg.ernet.in

Received 10 February 2012; Accepted 23 May 2012

ABSTRACT

In this work, biomass of *Hydrilla verticillata*, a waste weed was used in its immobilized form to remove hexavalent chromium from aqueous solutions. The powdered biomass was entrapped in polyvinyl alcohol and packed bed studies were carried out using beads of immobilized *H. verticillata*. Bed height, influent Cr(VI) concentrations, and influent flow rate were variable parameters for the present study. The overall performance of the biosorbent was satisfactory as very high Cr(VI) uptake (45.83 mg g^{-1}) was observed. Three different models—Bed depth service time (BDST), Yoon–Nelson, and Thomas—were studied and fitted to the experimental data. The correlation coefficient values were all above 0.96, whereas the BDST model fitted the data best. From the Thomas model, Thomas rate constant, K_{Th} was calculated and found to be $0.0215 \text{ L mg}^{-1} \text{ h}^{-1}$. The data obtained from the Yoon–Nelson model indicated that τ (148 min at 5 mg L^{-1}) values were very similar to experimental (140 min at 5 mg L^{-1}) results. Desorption studies of Cr(VI) were also carried out to find out the recovery of the metal ion.

Keywords: Biosorption; Heavy metal; *Hydrilla verticillata*; Packed bed; Kinetics; Wastewater treatment

1. Introduction

Biosorption may be simply defined as the removal of metal ions or organic compounds from their aqueous solutions by dead biomass. Biosorption provides the basis for a new technology for removal and recovery of especially heavy metals [1]. Biosorption was used since almost a decade to remove heavy metals from industrial wastewater, the purification of precious metals such as gold or silver, and the removal of organic pollutants from wastewater [2]. Metal removal by biosorption is a complex process and may include various processes such as adsorption, ion exchange, surface complexation, precipitation, etc. This process is

very promising as various types of dead biomasses make the sorption process technically more feasible and environment friendly [3]. The various advantages of biosorption include competitive performance, improved selectivity, low cost, regenerative, no sludge generation, and possibility of metal recovery [4]. Biosorption is an alternative to conventional physico-chemical methods of heavy metals removal such as precipitation, flocculation, ion exchange, membrane technologies, electrochemical treatment and catalytic reaction, etc. [5,6]. These processes are known to have high installation and operational costs and generate new products. These methods are not suitable especially when the dissolved metals are present in lower concentrations (less than 100 mg L^{-1}).

*Corresponding author.

Various studies were reported on the removal as well as recovery of precious metals such as gold, silver, palladium, and platinum, etc. [7]. The major factors which should be considered during metal biosorption are metal toxicity, metal cost and metal behavior. The majority of these studies were focused on dead biomass/biological material either in powder, granules, and/or beads forms. The use of nonliving powdered biomass in its native form for large-scale process is not feasible because of its smaller particle size, low mechanical strength, and difficulty of separation from the liquid stream due to relatively low density [8]. The industries that target for the use of metal biosorption process are mining, electroplating, coal-based power generation, and nuclear power generation [9,10]. Other industries like tanning, dyes and pigments, and metal finishing use chromium in their various operations [11].

Cr(VI) is being used in a variety of commercial processes in day-to-day life. Unregulated disposal of the chromium containing effluent in both developing and developed countries has led to the contamination of soil, sediment, surface, and ground waters [12]. Chromium is a chemical element and a member of group VI-B and it exists in the environment in many forms. Divalent chromium is relatively unstable, being rapidly oxidized to the trivalent form; thus, only two forms i.e. trivalent (Cr^{3+}) and hexavalent (Cr^{6+}) are found in nature. The hexavalent chromium is very toxic and carcinogenic, and thus it must be removed by converting it to less toxic trivalent form. The oxidation potential of hexavalent to trivalent chromium is strong and it is highly unlikely that oxidation of the trivalent form could occur *in vivo* [13].

Biosorption using low-cost biosorbents could be technically feasible and economically practical and is also a sustainable technology for the treatment of wastewater. In the literature, several studies were reported with different biosorbents for the removal of chromium(VI): activated sludge [14], saw dust, almond shell, wheat shell [15], tannery residual biomass [16], wool [17], bagasse, flyash [18], *Rhizopus nigrificans* [19], wallastonite [20], *Alligator* weed [21], *Terminalia arjuna* [22], *Eichhornia crassipes* [23], *Termitomyces clypeatus* [24], *Fagus orientalis* L [25], *Aeromonas caviae* [26], *Catla catla* scales [27], lignocellulosic residue [28], isolated microorganisms [29], granular activated carbon [30], and activated carbon from sugarcane bagasse [31].

In this paper, *Hydrilla verticillata*, a submerged aquatic weed was used as the biosorbent for the removal of Cr(VI) from aqueous solutions in a continuous up-flow packed bed reactor. *Hydrilla* can grow to the surface and form dense mats in all bodies of

water. It is native to the cool and warm waters of the world in Asia, Europe, Africa, and Australia. Temperature tolerance: *Hydrilla* is somewhat winter hardy; its optimum growth temperature is 20–27°C (68–81 F); the maximum temperature at which it can grow is 30°C (86 F). The accumulation and tolerance of Pb has been reported using *H. verticillata* by Gupta and Chandra [32]. The main aim of this work was to find out the extent of sorption of Cr(VI) from freshly prepared solutions onto the *H. verticillata* beads. Desorption studies were also carried out to find out the recovery of Cr(VI).

2. Materials and methods

2.1. Preparation of stock solution

A stock solution of Cr(VI) ($1,000 \text{ mg L}^{-1}$) was prepared by dissolving 2.826 g of $\text{K}_2\text{Cr}_2\text{O}_7$ in 1,000 mL deionized water, shaking it for 15 min at 120 rpm to obtain complete dissolution. Subsequent solutions of varying Cr(VI) concentrations were then obtained by diluting this stock solution. All the chemicals/reagents used in this study were of analytical reagent grade and purchased from Merck, Germany; S.D. Fine Chem. Ltd., India and Rankem, India.

2.2. Preparation of biomass

H. verticillata weeds were collected from a lake (freshwater) located inside the IIT Guwahati campus. Mature stems of *H. verticillata* were washed thoroughly with tap water to remove adhering water soaked soil and other soluble impurities on it. The washed stems were allowed to dry under sunlight for five days. Then the dried stems were kept in hot air oven at 70°C for 2 h for removing moisture content. The dried stems were then converted into fine powder by grinding in a ball mill. The powder was then sieved through 240 mesh in a screen seiver to obtain biosorbent with homogeneous particle size. These powdered biosorbent was then immobilized with polyvinyl alcohol (PVA).

Immobilized biomass beads were prepared using 30% (w/w) PVA. A known amount of biomass was mixed with PVA and the mixtures were constantly stirred at 100°C until the PVA gets dissolved. Trial experiments were carried out using various dosages of PVA ranging from 5 to 30% (w/w) and it was found that 30% (w/w) was the optimum PVA dose. These prepared beads were kept under sunlight for four days and also kept in hot air oven at a temperature of 70°C to remove moisture content. Dried beads were preserved in airtight polyethylene containers for further use.

2.3. Packed bed studies

A packed bed of 2.5 cm inner diameter and 50 cm height made up of perspex was used for sorption studies for the removal of chromium ions from aqueous solutions. The aqueous chromium ion solution was pumped in an upward direction through the packed bed by peristaltic pump at known flow rate. The samples were taken at predetermined time intervals and the concentrations of unadsorbed chromium ions were measured using UV–vis. spectrophotometer (Varian, Model Cary 50 Bio) by the diphenylcarbazide method (DCP) at wavelength of 540 nm.

The experiments were terminated when the bed got saturated. Three different bed heights (20, 40, and 50 cm) with the three different effluent concentrations (5, 20, and 50 mg L⁻¹) of Cr(VI) solutions were passed through the packed bed at different flow rates (10, 20, and 30 mL min⁻¹). Desorption studies were carried out immediately after the completion of adsorption. The continuous multiple experiments were carried out for both adsorption and desorption studies. The effluent was then collected and analyzed for Cr(VI) concentration. 1 N NaOH solution was used for the desorption studies. After completion of the desorption process, the bed was rinsed with deionized water till pH reached 6.5. During the experiment some precautions were taken viz: bed was kept in vertical position, no leakage of in and out flows of bed occurred and constant flow rate was maintained throughout the experiments. Before starting the experiment, beads were soaked in deionized water for 10 min to avoid channeling and to prevent the bubble formation inside the packed bed.

2.4. Analysis of packed bed data

Batch biosorption studies give only fundamental information related to the chromium biosorption performance of a given biosorbent. However, in industries, a continuous mode of operation is preferred and the breakthrough curves provide necessary informations for such operations. In the breakthrough curves, the normalized concentration, defined as the measured concentration divided by the inlet concentration and breakthrough is the plot of time vs. effluent concentration. Effluent volume (V_{eff}) is calculated from the following equation:

$$V_{\text{eff}} = Ft_e \quad (1)$$

The total quantity of Cr(VI) biosorbed in the packed bed (m_{ad}) is calculated from the area above the breakthrough curve (C vs. time) multiplied by the flow

rate (F). Dividing the Cr(VI) mass adsorbed (m_{ad}) by the biosorbent mass (M) leads to the uptake capacity (Q) of the biomass. The breakthrough time (t_b) was represented as the time at which the outlet Cr(VI) concentration reached 1 mg L⁻¹ and the bed exhaustion time (t_e) is the time at which the outlet Cr(VI) concentration exceeded 95% of that at the inlet. These breakthrough time and bed exhaustion time were used to evaluate the overall sorption zone (t) given by Eq. (2):

$$\Delta t = t_e - t_b \quad (2)$$

The length of the mass transfer zone (L_m) can be calculated from the breakthrough curve given by Eq. (3):

$$L_m = L \left(1 - \frac{t_b}{t_e} \right) \quad (3)$$

The total adsorbed metal quantity can be found out from the area under the breakthrough curve obtained by integrating the adsorbed concentration vs. time plot. Total adsorbed metal quantity in the packed bed for a given feed concentration and flow rate is calculated from the following equation:

$$m_{\text{ad}} = \frac{FA}{1000} \quad (4)$$

Total amount of metal sent to packed bed is calculated from the following equation:

$$m_{\text{total}} = \frac{C_o Ft_e}{1000} \quad (5)$$

Total removal percent of metal (packed bed performance) with respect to flow volume can also be found from the ratio of total adsorbed quantity of metal to the total amount of metal sent to the packed bed:

$$\text{Removal (\%)} = \frac{m_{\text{ad}}}{m_{\text{total}}} \times 100 \quad (6)$$

The metal mass desorbed (m_d) can be calculated from the area below the elution curve (C vs. time) multiplied by the flow rate. The desorption efficiency (E) can be calculated from Eq. (7):

$$E(\%) = \frac{m_d}{m_{\text{ad}}} \times 100 \quad (7)$$

Equilibrium metal uptake in the packed bed is defined by Eq. (8) as the total amount of metal sorbed per g of sorbent at the end of total flow time:

$$q_{\text{eq}} = \frac{m_{\text{total}}}{W} \quad (8)$$

and

$$C_x = \frac{1}{KC_b} \ln \left(\frac{C_o}{C_b} - 1 \right) \quad (12)$$

3. Modeling of the packed bed data

The design of a packed bed process requires prediction of the breakthrough curve and the maximum uptake capacity of a biosorbent. Various mathematical models were used in literature to describe fixed bed adsorption. In the present work, breakthrough curves obtained at different bed heights (Z), flow rates (F), and initial solute concentrations (C_o) were analyzed using three mathematical models viz. Bed depth service time (BDST), Thomas and Yoon–Nelson models.

3.1. BDST model with variation in flow rate

In packed bed systems, the main design principle is the service time of the bed, which means the time required by any adsorbent to remove a specified amount of impurity from solution before regeneration is required. The analysis of breakthrough curve was done using BDST model. BDST is a simple model for predicting the relationship between bed height, Z , and service time, t . The BDST model was based on the estimation of characteristic parameters such as the maximum adsorption capacity and kinetic constant. This model is used only for the description of the initial part of the break through curve i.e. up to the breakpoint or 10–50% of the saturation points [33].

$$\ln \left(\frac{C_o}{C_b} - 1 \right) = \ln \left(\exp \left(\frac{KN_o Z}{v} \right) - 1 \right) - KC_o t \quad (9)$$

In 1973, Hutchins [34] proposed a linear relationship between the bed depth and service time with the process variables is given by Eq. (10).

$$t_b = \frac{ZN_o}{C_o v} - \frac{1}{KC_b} \left(\frac{C_o}{C_b} - 1 \right) \quad (10)$$

where t_b is service time at breakthrough point, N_o is adsorption capacity per volume of bed (mg cm^{-3}), Z is the bed height of the packed bed (cm), C_o is the initial concentration of solute in the liquid phase (mg L^{-1}), v is linear flow rate (cm h^{-1}) defined as the ratio of the volumetric flow rate F (milliliters per hour) to the cross-sectional area of the bed S_c (cm^2), K is rate constant of adsorption ($\text{L mg}^{-1} \text{h}^{-1}$), and C_b is the breakthrough metal ion concentration (mg L^{-1}). Eq. (10) can be rewritten in the form of a straight line.

$$t_b = m_x Z - C_x \quad (11)$$

where m_x is slope of BDST line ($m_x = N_o / C_o v$) and the intercept of this equation represents as Eq. (12). Thus, N_o and K can be evaluated from slope (m_x) and the intercept (C_x) of the plot of t_b vs. Z , respectively.

3.2. Thomas model or reaction model

The Thomas model is one of the most common and extensively used model to predict the packed bed performance. The Thomas model assumes Langmuir kinetics, no axial dispersion and that the rate driving force obeys second-order reversible reaction kinetics. This model also assumes a constant separation factor which is applicable to either favorable or unfavorable isotherms. The weakness of this model is that its derivation is based on second-order reaction kinetics whereas many times it was found that adsorption is often controlled by interphase mass transfer. This inconsistency may lead to some error when this method is used to model adsorption process. The breakthrough curves were analyzed by using the Thomas model through the following Eq. (13) [35]:

$$\frac{C}{C_o} = \frac{1}{1 + \exp \left(\frac{k_{\text{TH}}}{F} (q_o M - C_o V_{\text{eff}}) \right)} \quad (13)$$

The linearized form of the Thomas model can be expressed as follows:

$$\ln \left(\frac{C_o}{C} - 1 \right) = \frac{k_{\text{TH}} q_o M}{F} - k_{\text{TH}} C_o t \quad (14)$$

where the kinetic coefficient (K_{TH}) and the maximum biosorption capacity (q_o) can be determined from a plot of $\ln[(C_o/C) - 1]$ against t at a given flow rate. C_o and C are metal ion concentrations (mg L^{-1}) in the influent and effluent, respectively, K_{TH} is the Thomas model rate constant ($\text{mL mg}^{-1} \text{min}^{-1}$), F is the flow rate (L h^{-1}), q_o is the maximum solid-phase concentration of the solute (mg g^{-1}), M is the total mass of the biosorbent loaded in the packed bed (g), and V_{eff} is the volume of metal solution passed through the packed bed (L).

3.3. Yoon and Nelson model

This model is based on assumption of the probability of adsorbate adsorption and breakthrough. The

Yoon and Nelson model not only is less complicated than other models, but also requires no detailed data regarding the characteristics of adsorbate, the type of adsorbent, and the physical properties of the bed. The Yoon and Nelson equation regarding to a single component system is expressed as [36,37]:

$$\frac{C}{C_0} = \frac{\exp(k_{YN}t - \tau k_{YN})}{1 + \exp(k_{YN}t - \tau k_{YN})} \quad (15)$$

The linear form of Yoon–Nelson model can be expressed as:

$$\ln\left(\frac{C}{C_0 - C}\right) = k_{YN}t - \tau k_{YN} \quad (16)$$

where K_{YN} is the rate constant (min^{-1}), τ is the time required for 50% adsorbate breakthrough (min), and t is the breakthrough (sampling) time (min). These values were determined from a plot of $\ln(C/(C_0 - C))$ vs. sampling time (t) according to Eq. (16). If the theoretical model accurately characterizes the experimental data, this plot will result in a straight line with slope of K_{YN} and intercept τK_{YN} [36,38]. The calculation of theoretical breakthrough curves for a single component system requires the determination of the parameters K_{YN} and τ for the adsorbate.

4. Results and discussion

The various physical properties of *H. verticillata* biomass are presented in Table 1. Continuous biosorption of heavy metals in packed bed is an efficient process as a very high degree of purification can be achieved in once through process. Usually, the performance of the packed bed is evaluated from the concept of breakthrough curve, which is obtained by plotting the measured concentration divided by the inlet concentration (C/C_0) against time (t). The breakthrough time (t_b), exhaustion time (t_e), Cr(VI) uptake, percentage removal, and critical bed length (Z) were calculated and presented in Table 2. It can be seen

from Table 2 that the breakthrough curve became flat as sorption progresses as a result of the decrease in breakthrough time and increase in exhaustion times. The overall performance of the biosorbent was very satisfactory as very high Cr(VI) uptake (45.83 mg g^{-1}) was observed.

4.1. Effect of bed height on biosorption of chromium

Breakthrough curves for biosorption of Cr(VI) by *H. verticillata* biomass at different bed heights are shown in Fig. 1 at 5 mg L^{-1} initial concentration. Experiments were carried out by keeping optimum operating conditions of biomass loading, residence time, and initial metal ion concentration at natural pH of the solution and ambient temperature. In order to yield different bed heights, 26.7, 70.5, and 93 g of biomass beads were added to produce 20, 40, and 50 cm packed bed height, respectively. From Fig. 1, it can be seen that for Cr(VI) metal ion, the breakthrough and exhaustion time increased with an increase in bed height as more free binding sites were available for sorption which resulted in a broadened mass transfer zone also (Table 2) [39]. This was mainly due to the higher contact time between metal ions solution and *H. verticillata* surface and also due to more number of active sites and ionic groups (surface functional groups) of biomass available for the sorption of chromium. The slope of the S-curve from t_b to t_e decreased as the bed height increased from 20 to 50 cm, which indicated that the breakthrough curve became steeper as the bed height decreased.

4.2. Effect of flow rates on biosorption

The breakthrough curves of Cr(VI) uptake for initial Cr(VI) concentrations of 5, 20, and 50 mg L^{-1} for different flow rates of 10, 20, and 30 mL min^{-1} for a packed bed depth of 50 cm were obtained (Figs. 2–4). It was noted that in the range of 10, 20, and 30 mL min^{-1} , the flow rate had very little effect on Cr(VI) uptake due to the fast sorption of Cr(VI) on the *H. verticillata*. In the batch process, the sorption reached equilibrium in less than 20 min, hence an appropriate flow rate could be chosen on the basis of making the process time efficient. The flow rate of 10, 20, and 30 mL min^{-1} was found to be suitable for optimum loading of the ion-association complex on the basic packed bed studies. At higher flow rates, there was a reduction in the percentage adsorption of chromium. This was due to the insufficient contact time between the Cr(VI) solution and the beads of *H. verticillata*. A flow rate of 10 mL min^{-1} was maintained for the elution of the metal ion.

Table 1
The physical characteristics of the *H. verticillata*

Parameters	Values
Bulk density (g/cm^3)	0.52
Particle density (g/cm^3)	0.72
BET surface area (m^2/g)	6.33
Porosity (%)	27.99
Pore volume (cm^3/g)	0.027
Moisture content (%)	11.68

Table 2

Calculated breakthrough time, exhaustion time, Cr(VI) uptake, percentage removal, and critical bed length

M (g)	Z (cm)	F (mL min ⁻¹)	C_o (Mg L ⁻¹)	t_e (min)	T (min)	L_m (cm)	m_{ad} (mg)	m_{tot} (mg)	R (%)	q_{eq} (mg g ⁻¹)	m_d (mg)	E (%)
93		10	5	140	125	44.64	3.208	7	45.83	0.075	2.408	75.06
93		20	5	100	90	45.00	4.915	10	49.15	0.107	3.315	67.44
93		30	5	80	70	43.75	4.525	12	37.71	0.129	2.125	46.96
93		10	20	130	120	46.15	8.567	26	32.95	0.279	7.767	90.66
93	50	20	20	100	80	40.00	10.880	40	27.21	0.430	9.287	85.30
93		30	20	70	60	42.85	7.281	42	17.33	0.451	4.881	67.03
93		10	50	130	110	42.30	12.75	65	19.62	0.698	11.950	93.72
93		20	50	80	70	43.75	17.040	80	21.30	0.860	15.440	90.61
93		30	50	60	50	41.66	20.570	90	22.86	0.967	18.170	88.33
70.5		10	5	120	100	33.33	2.925	6	48.76	0.085	2.125	72.65
70.5	40	20	5	90	70	31.11	3.916	9	43.51	0.127	2.316	59.14
70.5		30	5	70	60	34.28	3.468	10.5	33.03	0.148	1.068	30.79
26.7		10	5	110	100	18.18	2.537	5.5	46.13	0.205	1.737	68.46
26.7	20	20	5	70	50	14.28	2.514	7	35.91	0.262	0.914	36.35
26.7		30	5	50	30	12.00	2.545	7.5	33.94	0.280	0.145	5.72

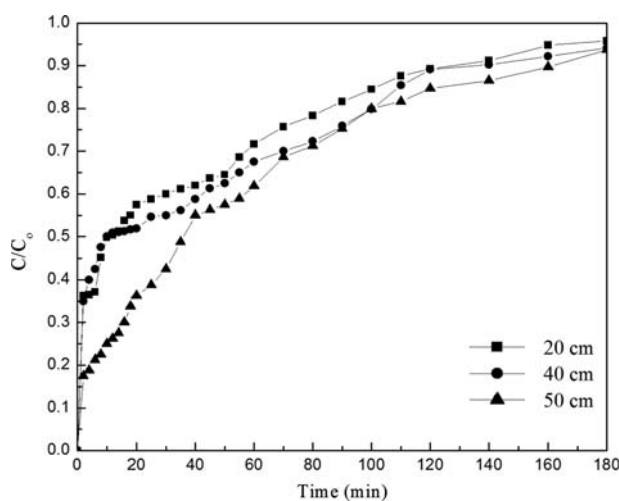


Fig. 1. Breakthrough curves for Cr(VI) removal at various packed bed heights at 30 mL min⁻¹ flow rate and initial metal ion concentration 5 mg L⁻¹.

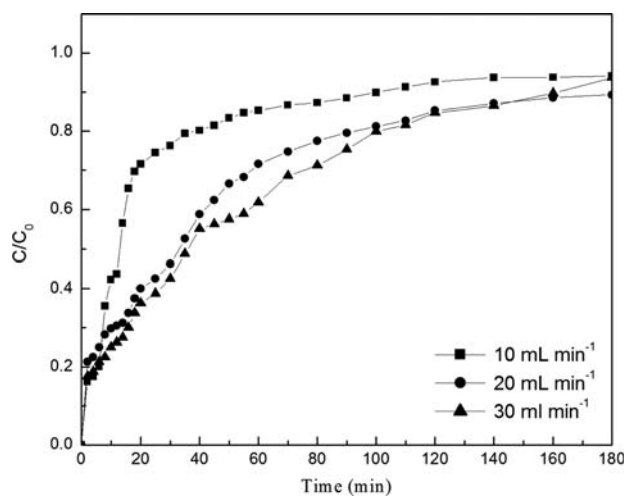


Fig. 2. Breakthrough curves for Cr(VI) removal at various flow rates, initial metal concentration of 5 mg L⁻¹, and 50 cm bed height.

4.3. Effect of initial metal ion concentration on biosorption

Three different initial Cr(VI) concentrations (5, 20, and 50 mg L⁻¹) were used, while keeping the bed height and flow rate constant. As observed in the Fig. 5, the breakthrough and exhaustion times decreased with increasing initial Cr(VI) concentration, as a high concentration lead to rapid saturation of the biomass and earlier packed bed stoppage. This ultimately lead to steeper breakthrough curves, as observed in Table 2. Maximum Cr(VI) uptakes were

obtained for the lowest initial Cr(VI) concentration. The Cr(VI) ion removal efficiency decreased with increasing initial Cr(VI) ion concentration. This could be attributed to the fact that at low solute concentrations, the surface functional groups on the biosorbent may be sufficient to accommodate all the solute molecules, i.e. fractional sorption becomes independent of the initial solute concentration. With increasing solute concentration, the number of availability of such sites became fewer compared to the Cr(VI) ions present; hence, the percentage of Cr(VI) removal decreased.

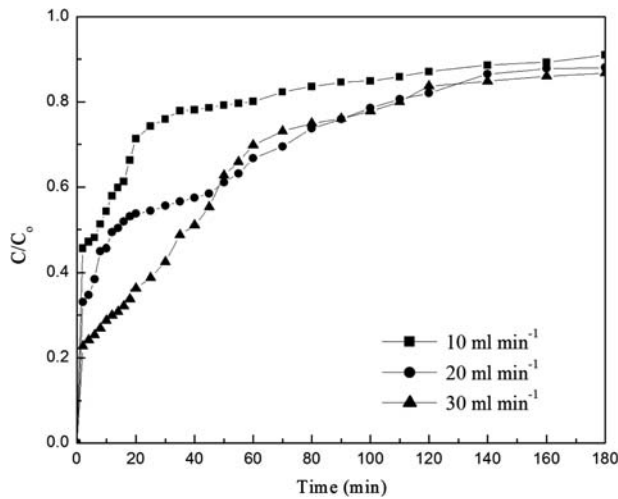


Fig. 3. Breakthrough curves for Cr(VI) removal at various flow rates, initial metal concentration of 20 mg L^{-1} , and 50 cm bed height.

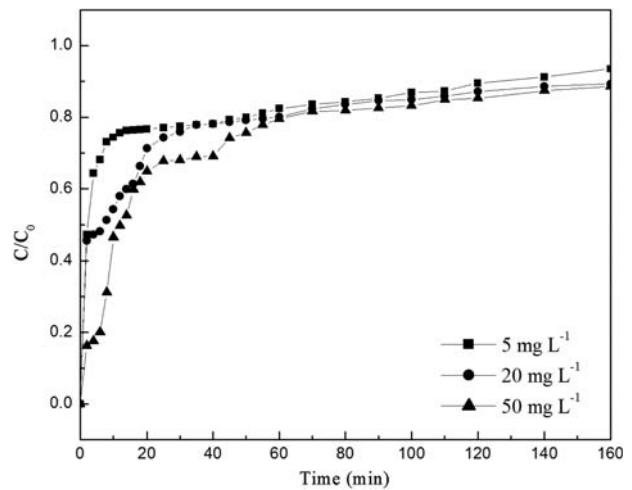


Fig. 5. Breakthrough curves for Cr(VI) removal at various initial metal ion concentrations 10 mL min^{-1} flow rate and 50 cm bed height.

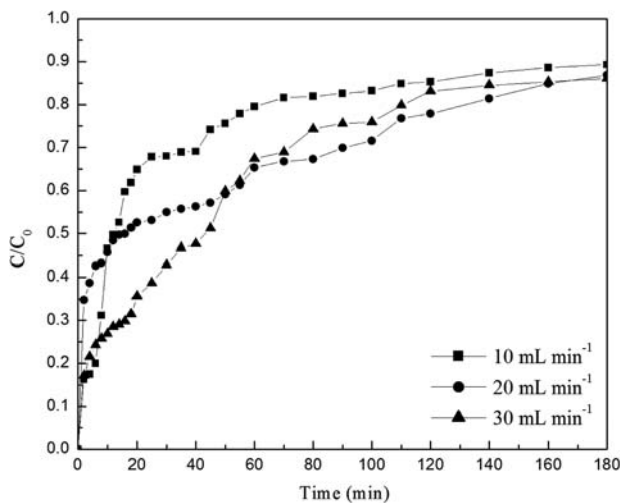


Fig. 4. Breakthrough curves on Cr(VI) removal at various flow rates, initial metal concentration of 50 mg L^{-1} , and 50 cm bed height.

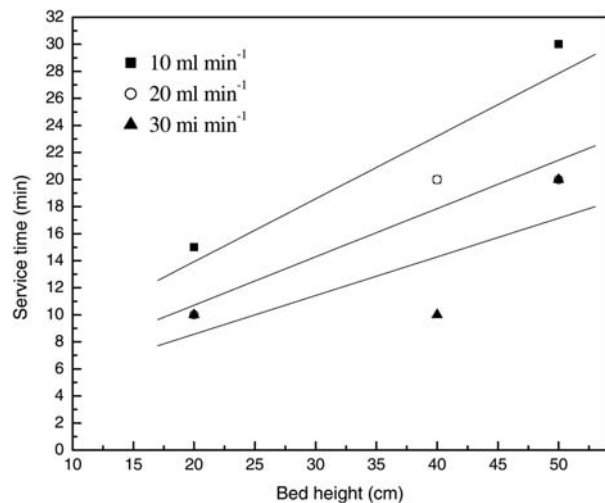


Fig. 6. BDST plot for Cr(VI) adsorption at various breakthroughs.

4.4. Bed depth service time model

From Eq. (10), breakthrough service time (t_b) and bed depth results are plotted in Fig. 6. The experiments were carried out for packed bed depth of 20, 40, and 50 cm only. By using Eq. (12), slope, intercepts, and correlation coefficients were calculated by plotting service time vs. bed depth and results are shown in Table 3. From Table 3, it can be seen that correlation coefficient values are all above 0.96 suggesting that BDST model fitted the data well. There was also a consistent rise in slopes from 0.285 to 0.464 from breakthrough and subsequent increase in corresponding dynamic adsorption capacity N_0 from 0.354 to 0.654 mg L^{-1} . At lower breakthrough value,

some active sites of the biosorbent were still unoccupied by metal ions and thus the adsorbent remained unsaturated. This indicates that the dynamic adsorption capacity in such low breakthrough condition will be lower than the full bed capacity of the adsorbent.

4.5. The Thomas model

The data obtained in packed bed studies were fitted to the Thomas model to determine the Thomas rate constant (K_{TH}), equilibrium specific uptake of chromium (q_0) and were used to predict the breakthrough curve for the dynamic sorption of chromium. The data obtained from the model clearly indicated that the linearized Thomas equation adequately

Table 3
Coefficients of BDST equation at different breakthrough

F (ml min ⁻¹)	Z (cm)	t_b (min)	N_o (Mg L ⁻¹)	C_b (mg L ⁻¹)	K_a (L mg ⁻¹ h ⁻¹)	R^2
10	20	15	0.354	1.5	0.014	0.862
	40	20	0.354	3.62	0.010	0.862
	50	30	0.354	4.25	0.010	0.862
20	20	10	0.540	1.43	0.019	0.964
	40	20	0.540	3.12	0.015	0.964
	50	20	0.540	3.06	0.015	0.964
30	20	10	0.654	1.25	0.025	0.571
	40	10	0.654	2.18	0.021	0.571
	50	20	0.654	2.59	0.020	0.571

described the experimental breakthrough sorption data. A linear regression was then performed on each set of transformed data to determine the coefficients from slope and intercept. The values of K_{Th} and q_o are presented in Table 4. It can be seen that as the flow rate increased from 10, 20, and 30 mL min⁻¹, the Thomas rate constant increased and the specific uptake of chromium decreased for the chromium concentrations studied. The bed capacity q_o increased and the coefficient K_{Th} decreased with increasing inlet metal ion concentration. The data in Table 4, also show a small difference between the experimental and predicted values of the bed capacity (q_o) obtained at all inlet Cr(VI) concentrations studied, although the deviations of experimental data from predicted values are evident at three different flow rates. The Thomas model is suitable for adsorption processes where the external and internal diffusions will not be the limiting step [33].

4.6. The Yoon–Nelson model

A simple theoretical model developed by Yoon–Nelson in 1984 [36] was applied to investigate the breakthrough behavior of metal ions. The values of

K_{YN} (a rate constant) and τ (the time required for 50% adsorbate breakthrough) were determined from $\ln[C/(C_o - C)]$ against t plots at three different flow rates 10, 20, and 30 mL min⁻¹ and at three different inlet Cr (VI) concentrations of 5, 20, and 50 mg L⁻¹. These values were used to calculate the breakthrough curve. The values of K_{YN} and τ are calculated and also listed in Table 5. From Table 5, it can be seen that the rate constant K_{YN} increased and τ decreased with both increasing flow rate and Cr(VI) inlet concentration. The data in Table 5 also indicate that τ values are very similar to experimental results and comparison of the experimental and predicted breakthrough curves obtained at different flow rates according to the Yoon–Nelson model. From the experimental results and data regression, the model proposed by Yoon–Nelson provided a good correlation of the effects of inlet Cr(VI) concentration and flow rate.

5. Desorption and recovery

The possibility of adsorbent regeneration (desorption) and metal recovery was primarily studied based on the general assumption that regeneration of adsorbent is directly linked to the economics of the

Table 4
Parameters predicted from the Thomas model at 50 cm bed height, different concentrations, and different flow rates

C_o (mg L ⁻¹)	F (ml min ⁻¹)	K_{Th} (mL/min mg)	$q_{o,theo}$ (mg g ⁻¹)	$q_{o,exp}$ (mg g ⁻¹)	R^2
5	10	0.0014	3.125	3.208	0.901
20		0.00045	7.923	8.567	0.855
50		0.0002	13.54	12.75	0.717
5	20	0.0018	4.575	4.915	0.786
20		0.00055	11.72	10.88	0.742
50		0.00026	16.81	17.04	0.706
5	30	0.0022	4.976	4.552	0.911
20		0.00065	12.85	7.281	0.966
50		0.00032	18.11	20.57	0.783

Table 5

Parameters predicted from the Yoon–Nelson model at 50 cm bed height, different concentrations, and different flow rates

C_0 (mg L ⁻¹)	F (ml min ⁻¹)	K_{YN} (L min ⁻¹)	τ_{theo} (min)	τ_{exp} (min)	R^2
5	10	0.007	148.1	140	0.901
20		0.009	93.88	110	0.855
50		0.01	64.2	90	0.717
5	20	0.009	108.4	100	0.786
20		0.011	69.45	90	0.742
50		0.013	39.84	60	0.706
5	30	0.011	78.63	80	0.911
20		0.013	50.76	70	0.966
50		0.016	28.62	50	0.783

process. In a previous study, Sudha and Abraham [19] have noticed that solutions of alkali and highly alkaline salts (NaOH, Na₂CO₃, and NaHCO₃) were better eluting agents than acids or mineral salts for Cr(VI) desorption from immobilized fungal biomass. Continuous desorption of Cr(VI) from *Sphagnum* moss peat studied by Sharma and Forster [39] using 1 M NaOH was another example that favored alkaline desorption. From this study, it appears that higher concentration of NaOH may be required to increase the Cr (VI) desorption efficiency. The study with more concentrated NaOH solutions was not pursued further as the resulting treatment cost would further increase. The recovery of metal ions from the metal saturated bed is an important step towards further reducing the process cost.

Before starting the desorption experiment, one adsorption experiment was carried out with three packed bed heights of 20, 40, and 50 cm initially fed with 5 mg L⁻¹ Cr(VI) concentration at 10 mL min⁻¹

flow rate till exhaust. The exhausted adsorbent bed was used for desorption study. Desorption study was conducted with desorbent of 1 M NaOH at lower flow rate than adsorption. Lower flow rate was applied so as to allow more contact time and concentrate the chromate ions in possible minimum volume. A time of desorbent vs. normalized concentration (C/C_0) of chromium recovered is shown in Fig. 7 with different Cr(VI) concentrations (5, 20, and 50 mg L⁻¹) and 40 cm bed height and 10 mL min⁻¹. From the figure, effluent total chromium concentration was observed to be decreased as the time elapsed. Corresponding desorption and elution efficiencies are shown in Table 2.

6. Conclusion

In this work, an extensive lab scale investigation was conducted to evaluate packed bed performance for the removal of hexavalent chromium from aqueous solution. *H. verticillata* immobilized with PVA was used as the adsorbent in the packed bed. Bed height, influent Cr(VI) concentrations, and influent flow rate were variable parameters for the present study. The data obtained for Cr(VI) were well described by BDST breakthrough equation. Adsorption rate constant and dynamic bed capacity at 10% breakthrough were observed to be 0.0215 L mg⁻¹ h⁻¹ and 0.654 mg L⁻¹, respectively. Critical bed depth of adsorbent that would be able to prevent the chromium concentration from exceeding the permissible limit was obtained as 50 cm at flow rate of 5 mL min⁻¹ and initial Cr(VI) 5 mg L⁻¹. The Thomas and the Yoon–Nelson models were applied to experimental data obtained from dynamic packed bed studies. The model constants belonging to each model were determined by linear and nonlinear regression techniques and were proposed for the use in packed bed design. It seems that although the immobilization process decreased the Cr(VI) biosorption properties of the biomass, *H. verticillata* has a considerable potential for the removal of Cr(VI) over a

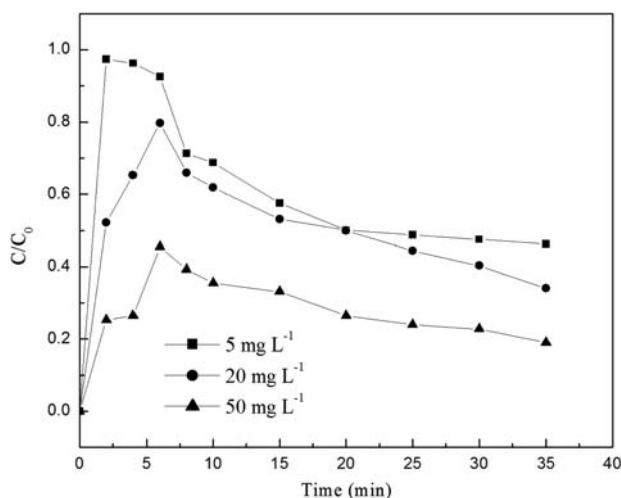


Fig. 7. Desorption profile for Cr(VI) at different concentrations, 40 cm bed height, and 10 mL min⁻¹ flow rate.

lower range of Cr(VI) concentration. The results also indicated that the sorption process could only deal with lower flow rates and lower concentrations of Cr(VI) solutions if a high percentage removal was required for extended periods. By adjusting the operating characteristics of the packed bed, such as the flow rate, inlet Cr(VI) concentration, and biomass quantity very rapid and an effective chromium uptake can be achieved for the system.

References

- [1] B. Volesky, *Biosorption of Heavy Metals*, CRC Press, Boca Raton, FL, 1990, pp. 396–401.
- [2] G.M. Gadd, Biosorption: critical review of scientific rationale, environmental importance and significance for pollution treatment, *J. Chem. Technol. Biotechnol.* 84 (2009) 13–28.
- [3] G.M. Gadd, Biosorption, *J. Chem. Technol. Biotechnol.* 55 (1992) 302–305.
- [4] A. Sari, M. Tuzen, Biosorption of total chromium from aqueous solution by *red algae (Ceranium virgatum)*: equilibrium, kinetic and thermodynamic studies, *J. Hazard. Mater.* 160 (2008) 349–355.
- [5] D. Kratochvil, B. Volesky, Advances in the biosorption of heavy metal, *Rev. Tibtech.* 16 (1998) 291–300.
- [6] F.J. Alguacil, I. Garcia-Diaz, Felix Lopez, The removal of chromium (III) from aqueous solution by ion exchange with Amberlite 200 resin: batch and continuous ion exchange modelling, *Desalin. Water Treat.* 45 (2012) 55–60.
- [7] N. Das, Recovery of precious metals through biosorption—A review, *Hydrometallurgy* 103 (2010) 180–189.
- [8] M. Tsezos, Adsorption by microbial biomass as a process for removal of ions from process or waste solutions, in: H. Eccles, S. Hunt (Eds.), *Immobilization of Ions by Biosorption*, Ellis Horwood, Chichester, 1986, pp. 201–218.
- [9] M.Y. Arica, G. Bayramoglu, Cr(VI) biosorption from aqueous solutions using free and immobilized biomass of *Lentinus sajor-caju*: Preparation and kinetic characterization, *Colloids Surf. A: Physicochem. Eng. Aspects* 253 (2005) 203–211.
- [10] B. Volesky, Biosorption and me, *Water Res.* 41 (2007) 4017–4029.
- [11] N.R. Bishnoi, M. Bajaj, N. Sharma, A. Gupta, Adsorption of Cr(VI) on activated rice husk carbon and activated alumina, *Bioresour. Technol.* 91 (2004) 305–307.
- [12] M.D. Szulczewski, P.A. Helmke, W.F. Bleam, Comparison of XANES analysis and extractions to determine chromium speciation in contaminated soils, *Environ. Sci. Technol.* 31 (1997) 2954–2959.
- [13] H.A. Schroeder, J.J. Balassa, I.H. Tipton, Abnormal trace metals in man—chromium, *J. Chron. Dis.* 15 (1962) 941–964.
- [14] A. Zümriye, A. Derya, Competitive biosorption of phenol and chromium(VI) from binary mixtures onto dried anaerobic activated sludge, *Biochem. Eng. J.* 7 (2001) 183–193.
- [15] M. Dakiky, M. Khamis, A. Manassra, M. Mereb, Selective adsorption of Cr(VI) in industrial wastewater using low cost abundantly available adsorbents, *Adv. Environ. Res.* 6 (2002) 533–540.
- [16] P.D. Saha, A. Dey, P. Marik, Batch removal of chromium (VI) from aqueous solutions using wheat shell as adsorbent: Process optimization using response surface methodology, *Desalin. Water Treat.* 39 (2012) 95–102.
- [17] J. Anandkumar, B. Mandal, Adsorption of chromium(VI) and Rhodamine B by surface modified tannery waste: Kinetic, mechanistic and thermodynamic studies, *J. Hazard. Mater.* 186 (2011) 1088–1109.
- [18] M. Rao, A. Parawate, A. Bhole, Removal of Cr(VI) and Ni(II) from aqueous solution using bagasse and fly ash, *Waste Manage.* 22 (2002) 821–830.
- [19] B.R. Sudha, T.E. Abraham, Studies on enhancement of Cr(VI) biosorption by chemically modified biomass of *Rhizopus nigricans*, *Water Res.* 36 (2002) 1224–1236.
- [20] Y. Sharma, Cr(VI) removal from industrial effluents by adsorption on an indigenous low cost material, *Colloids Surf. A* 215 (2003) 155–162.
- [21] X.S. Wang, Y.P. Tang, R.T. Sheng, Kinetics, equilibrium and thermo dynamics study on removal of Cr(VI) from aqueous solutions using low cost adsorbent *Alligator weed*, *Chem. Eng. J.* 148 (2008) 217–225.
- [22] K. Mohanty, J. Mousam, B.C. Meikap, M.N. Biswas, Removal of chromium (VI) from dilute aqueous solutions by activated carbon developed from *Terminalia arjuna* nuts activated with zinc chloride, *Chem. Eng. Sci.* 60 (2005) 3049–3059.
- [23] K. Mohanty, J. Mousam, B.C. Meikap, M.N. Biswas, Biosorption of Cr(VI) from aqueous solutions by *Eichhornia crassipes*, *Chem. Eng. J.* 117 (2006) 71–77.
- [24] S.K. Das, A.K. Guha, Biosorption of chromium by *Termitomyces clypeatus*, *Colloids and Surf. B* 60 (2007) 46–54.
- [25] F.N. Acar, E. Malkoc, The removal of chromium(VI) from aqueous solutions by *Fagus orientalis* L, *Bioresour. Technol.* 94 (2004) 13–15.
- [26] M.X. Loukidou, A.I. Zouboulis, T.D. Karapantsios, K.A. Matis, Equilibrium and kinetic modeling of chromium(VI) biosorption by *Aeromonas caviae*, *Colloids Surf. A* 242 (2004) 93–104.
- [27] K. Srividya, K. Mohanty, Biosorption of hexavalent chromium from aqueous solutions by *Catla catla scales*: Equilibrium and kinetics studies, *Chem. Eng. J.* 155 (2009) 666–673.
- [28] T.S. Anirudhan, S. Rijith, C.D. Bringle, Iron(III) complex of an amino-functionalized Poly(acrylamide)-grafted lignocellulosic residue as a potential adsorbent for the removal of chromium (VI) from water and industry effluents, *Desalin. Water Treat.* 12 (2009) 3–15.
- [29] T. Mandal, D. Dasgupta, S. Datta, A biotechnological thrive on COD and chromium removal from leather industrial wastewater by the isolated microorganisms, *Desalin. Water Treat.* 13 (2010) 382–392.
- [30] P.D. Chandra, J.N. Sahu, C.R. Mohanty, B. Raj Mohan, B.C. Meikap, Column performance of granular activated carbon packed bed for Pb(II) removal, *J. Hazard. Mater.* 156 (2008) 596–603.
- [31] K.J. Cronje, K. Chetty, M. Carsky, J.N. Sahu, B.C. Meikap, Optimization of chromium(VI) sorption potential using developed activated carbon from sugarcane bagasse with chemical activation by zinc chloride, *Desalination* 275 (2011) 276–284.
- [32] M. Gupta, P. Chandra, Lead accumulation and toxicity in *Valisneria spiralis* and *Hydrilla verticillata* (l. f.) Royle, *J. Environ. Sci. Health A* 29 (1994) 703–516.
- [33] G.S. Bohart, E.Q. Adams, Some aspects of behaviour of charcoal with respect to chlorine, *J. Am. Chem. Soc.* 42 (1920) 523–529.
- [34] R.A. Hutchin, New simplified design of activated carbon systems, *Am. J. Chem. Eng.* 80 (1973) 133–138.
- [35] H.C. Thomas, Heterogeneous ion exchange in a flowing system, *J. Am. Chem. Soc.* 66 (1994) 1664–1666.
- [36] Y.H. Yoon, J.H. Nelson, Application of gas adsorption kinetics: i. a theoretical model for respirator cartridge service life, *Am. Ind. Hyg. Assoc. J.* 45 (1984) 509–516.
- [37] Y.H. Yoon, J.H. Nelson, Application of gas adsorption kinetics: ii. a theoretical model for respirator cartridge service life and its practical applications, *Am. Ind. Hyg. Assoc. J.* 45 (1984) 517–524.
- [38] W.T. Tsai, C.Y. Chang, C.Y. Ho, L.Y. Chen, Adsorption properties and breakthrough model of 1,1-dichloro-1-fluoroethane on activated carbons, *J. Hazard. Mater.* 69 (1999) 53–66.
- [39] D.C. Sharma, C.F. Forster, Continuous adsorption and desorption of chromium ions by *Sphagnum moss peat*, *Process Biochem.* 30 (1995) 293–298.